CHEMISTRY
A EUROPEAN JOURNAL

DOI: 10.1002/chem.200501242

Metal Nuclearity Modulated Four-, Six-, and Eight-Connected Entangled Frameworks Based on Mono-, Bi-, and Trimetallic Cores as Nodes

Xin-Long Wang,[a] Chao Qin,[a] En-Bo Wang,*[a] and Zhong-Min Su*[b]

Abstract: To investigate the relationship between network connectivity and metal nuclearity, we designed and synthesized a series of three-dimensional (3D) entangled coordination frameworks based on different metal cores, namely $[Zn_2(bdc)_2(L)_2]\cdot 2H_2O$ (**1**), $[Zn(bdc)(L)_{0.5}]$ (**2**), $[Zn(oba)(L)_{0.5}]$ (**3**) and $[Cd_3(bdc)_3(L)_2(H_2O)_2]$ (**4**) by self-assembly of d^{10} metal salts with the flexible long-chain ligand 1,4-bis(1,2,4-triazol-1-yl)butane (L), and with the rigid and nonrigid aromatic dicarboxylate ligands 1,4-benzenedicarboxylate (bdc) and 4,4′-oxybis(benzoate) (oba). Compound **1** exhibits a threefold interpenetrated diamondoid array typically based on a tetrahedral second building unit (SBU) at a single Zn center. Compound **2** adopts a threefold interpenetrated α-polonium-type network that is built from bimetallic cores as six-connected vertices. The structure of **3** also consists of dinuclear units; it comprises a novel (3,4)-connected threefold interpenetrated net with complex $(4\cdot6\cdot10)(4\cdot6^2\cdot10^3)$ topology when single zinc centers act as four-connected nodes (or the α-Po topology if dinuclear units are considered as six-connected nodes). Compound **4**, derived from a cross-linked fivefold interpenetrated diamond-like substructure, is an unusual example of a self-penetrating coordination framework displaying an unprecedented eight-connected $4^{20}6^8$ topology with trinuclear cadmium clusters as eight-connected nodes which, to our knowledge, not only defines a new topology for eight-connected coordination networks, but also represents the highest connected topology presently known for self-penetrating systems. Detailed structural comparison of these complexes indicates that the increase in metal nuclearity induces the progressive increase in the connectivities of the ultimate nets: that is, the metal nuclearity plays a significant role in tuning the connectivity of a specific network. The thermal and luminescent properties of these compounds are discussed.

Keywords: coordination modes · coordination polymers · entangled networks · self-assembly · supramolecular chemistry

Introduction

Current interest in polymeric coordination networks is rapidly expanding owing to their intriguing architectures and potential applications,[1,2] although true crystal engineering of coordination polymers (that is, prediction of the precise solid-state structure) still remains a long-term challenge for the crystal engineer. Entangled systems, one of the major themes of supramolecular chemistry, are common in biology—as seen in catenanes, rotaxanes, and molecular knots[3]—and have attracted considerable attention due to their aesthetic and often complicated architectures and topologies.[4] There are two comprehensive reviews by Robson and Batten[5] of interpenetration, which has been the most investigated type of entanglement. More recently, all the 3D interpenetrated structures contained in the CSD database underwent a complete analysis with a rationalization and classification of the topology of the interpenetration.[6] According to Batten and Robson, interpenetrating network structures, which "can be regarded as infinite, ordered polycatenanes or polyrotaxanes",[5a] are characterized by the presence of two or more independent networks that are inextricably entangled through the rings belonging to one

[a] Dr. X.-L. Wang, Dr. C. Qin, Prof. E.-B. Wang
Institute of Polyoxometalate Chemistry
Department of Chemistry
Northeast Normal University
Changchun, Jilin 130024 (China)
Fax: (+86) 431-509-8787
E-mail: wangenbo@public.cc.jl.cn

[b] Prof. Z.-M. Su
Institute of Functional Materials
Department of Chemistry
Northeast Normal University
Changchun, Jilin, 130024 (China)
Fax: (+86) 431-509-8787
E-mail: zmsu@nenu.edu.cn

Supporting information for this article is available on the WWW under http://www.chemeurj.org/ or from the author.

framework. Remarkably, if *n*-fold interpenetrating networks are connected through bridging molecules, another intriguing type of entanglement can be achieved, that is, self-penetration, which, in contrast to interpenetrating nets, is a single network having the peculiarity that the smallest topological rings are catenated by other shorter rings belonging to the same net. This feature is not very common within coordination polymers and only a limited number of self-penetrated nets have been reported to date.[7]

Apart from their intrinsic aesthetic appeal, interest in entangled structures has been heightened by the fact that their resulting overall architectures are more flexible than the usual networks based entirely on coordination bonds[8]. This is a functional property that has potential applications ranging from drug delivery vehicles to sensor devices.[9] Therefore, the exploitation of such species will not only increase the vast structural diversity for coordination polymers, but also provide new insights into the study of the relationships between structure and function in these materials.

Ongoing research in our laboratory has been directed toward the design and synthesis of novel entangled networks.[10] Conformationally nonrigid ligands are usually the typical building elements for the assembly of interesting entangled structures, thanks to their varied geometries.[11] As an extension of our previous work, for our synthetic strategy we first chose a flexible long-chain ligand, 1,4-bis(1,2,4-triazol-1-yl)butane (L), whose coordination chemistry, to the best of our knowledge, had not been investigated previously. However, the construction of polynuclear metal clusters through the hydrolysis of metal salts in the presence of carboxylate ligands has been of concurrent interest.[12] Topologically these metal clusters have great potential in building highly connected metal–organic frameworks, since they are larger and have more coordination sites but cause less steric hindrance when coordinated with organic ligands. Unfortunately, although quite fascinating metal-cluster-based 3D structures have been documented,[13] no systematic investigation of the relationship between network connectivity and metal nuclearity has yet been reported. An understanding of the effect induced by metal nuclearity may therefore assist toward the rational design of diversely connected metal–organic frameworks. For this purpose, comparison of a series of related structures based on different nuclear metals is required. Fortunately, this has been achieved successfully for four entangled coordination polymers by simultaneous use of the flexible long-chain ligand L and aromatic dicarboxylate ligands having bridging ability (bdc = 1,4-benzenedicarboxylate; oba = 4,4′-oxybis(benzoate)), namely, $[Zn_2(bdc)_2(L)_2]\cdot 2H_2O$ (**1**), $[Zn(bdc)(L)_{0.5}]$ (**2**), $[Zn(oba)(L)_{0.5}]$ (**3**), and $[Cd_3(bdc)_3(L)_2(H_2O)_2]$ (**4**) built upon mono-, bi- and trimetallic cores, respectively. The crystal structures of these compounds and topological analyses, along with the systematic investigation of the modulated effect of metal nuclearity and coordination modes of carboxylate ligands on the ultimate framework topologies, will be represented and discussed in this paper.

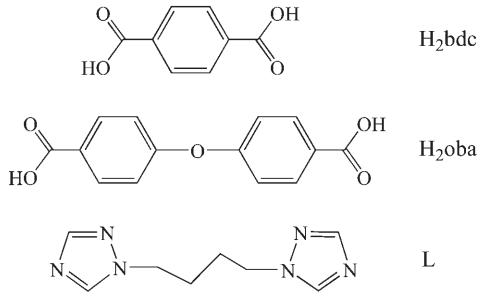

Results

Crystal structures: Single-crystal X-ray structural analysis reveals that the structure of **1** contains two crystallographically unique (but chemically and topologically identical) Zn atoms, two bdc, and two L ligands. The ORTEP view of the local coordination geometries around the Zn atoms is shown in Figure 1. Each Zn^{II} lies on a center of symmetry and is coordinated with two *trans* L ligands via nitrogen atoms (Zn–N 2.009(4)–2.059(4) Å) and two *trans* bdc ligands via carboxylic oxygen atoms (Zn–O 1.936(4)–2.002(5) Å). The bridges formed by L and bdc ligands do not sit in a plane; based on the second building unit (SBU) concept, two carboxylate oxygen atoms and two triazolyl nitrogen atoms in each Zn center constitute a tetrahedral SBU (Figure 2, left). The extension of the structure into a 3D network is accomplished by connecting four linear li-

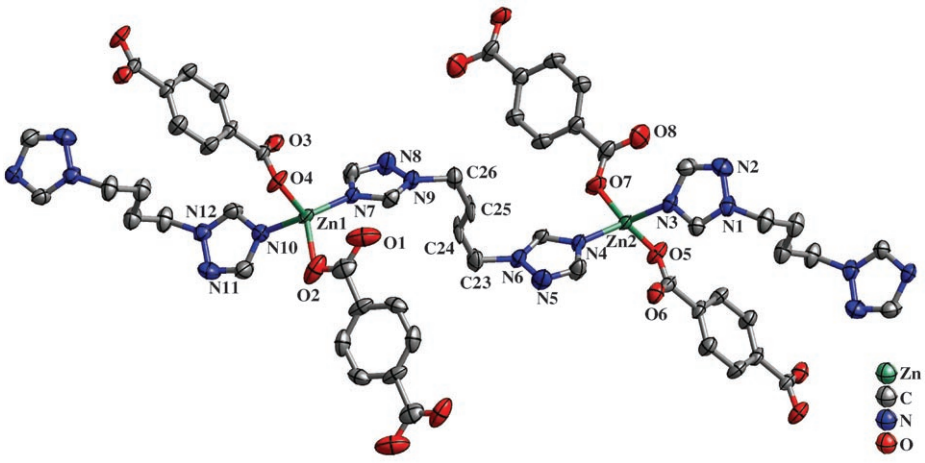

Figure 1. ORTEP diagram showing the coordination environments for Zn atoms in **1**.

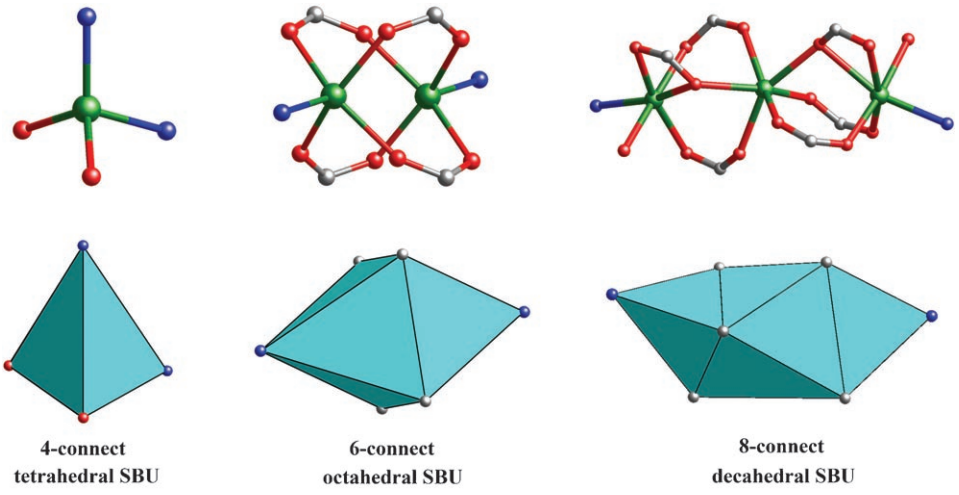

Figure 2. Schematic representation of inorganic SBUs.

gands to the tetrahedral building block (see Figure S1 in the Supporting information). The topological analysis of **1** reveals that it is a typically diamondoid framework containing large adamantanoid cages; Figure 3 also shows a single cage

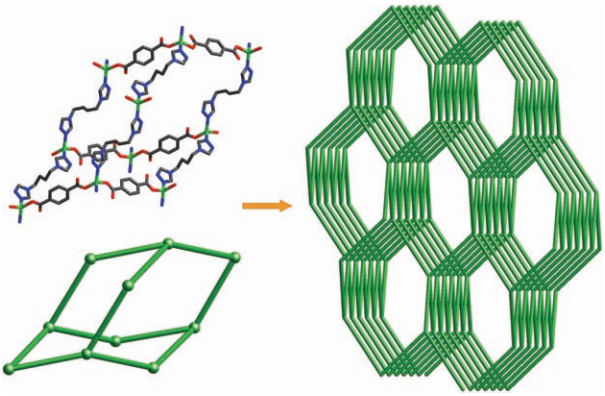

Figure 3. Single adamantanoid cages (left) and a schematic view of a single diamond-like framework (right).

delimited by four cyclohexane-like windows in chair conformation. As can be seen, the adamantanoid cages are elongated significantly in one direction, and exhibit maximum dimensions (corresponding to the longest intracage Zn···Zn distances) of 17.54 Å × 38.05 Å × 18.29 Å. Because of the spacious nature of the single network, it allows two identical diamondoid networks to interpenetrate it in a normal mode giving rise to a threefold interpenetrating dia array (see Figure 4), with isolated water molecules occupying the neutral channels (see Figure S2 in the Supporting information). The L ligands in **1** display three distinct conformations owing to the long and flexible alkyl chain, giving three pairs of different N–N and metal–metal distances (N–N 8.79 Å, Zn···Zn 12.41 Å; N–N 8.56 Å, Zn···Zn 11.64 Å; N–N 8.40 Å, Zn···Zn 11.28 Å). This flexible coordination feature has been observed in two polymeric complexes with a related ligand 1,3-bis(1,2,4-triazol-1-yl)propane (btp),[14] $Cu(btp)_2(CH_3CN)(H_2O)](CF_3SO_3)_2$, and $[Co(btp)_2(NCS)_2]_n$, in which btp ligands bridge metal atoms in 1D or 2D structures rather than 3D frameworks due to the introduction of capping groups. An analysis of the topology of interpenetration according to a recent classification[6] reveals that **1** belongs to Class Ia (all the interpenetrated nets are generated only by translation and the translating vector is [010] (11.32) Å). As often observed in interpenetrated diamondoid network structures, close π–π contacts[15] occur between triazolyl and aromatic rings (parallel stacking with distances face–face of 3.38 Å and 3.52 Å, centroid–centroid of 3.90 Å and 3.98 Å, and lateral offset of 1.78 Å and 1.97 Å), whereby they stabilize the solid-state structures.

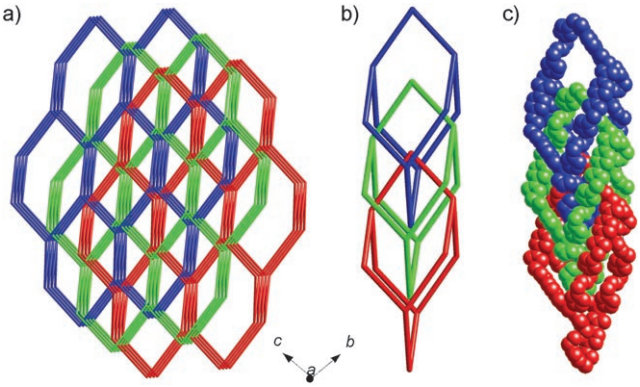

Figure 4. a) Three interpenetrating diamond-like nets in **1**; b) three interpenetrating adamantanoid cages; c) space-filling diagram of the three interpenetrating adamantanoid cages.

Compound **2**, obtained by changing the reaction conditions, adopts a threefold interpenetrated 3D network structure of α-Po topology that is built from dinuclear Zn_2 units with a paddle-wheel structure. Figure 5 illustrates the coordination environment of the Zn atoms and the sixfold connectivity of the bimetallic unit. Each Zn^{II} atom in the dinuclear motif is coordinated by four carboxylic oxygen atoms of bdc ligands (Zn–O 2.0445(16)–2.0670(16) Å) and one nitrogen atom of an L ligand (Zn–N 2.0145(18) Å) to furnish a square-pyramidal geometry. Two crystallographically equivalent Zn^{II} atoms are bridged by four carboxylates bonded in the bridging bis(bidentate) fashion to give a paddle-wheel shaped $[Zn_2(CO_2)_4]$ fragment in which the Zn···Zn distance is 2.980(3) Å. The axis sites of each Zn_2 paddle wheel are occupied by two additional L ligands

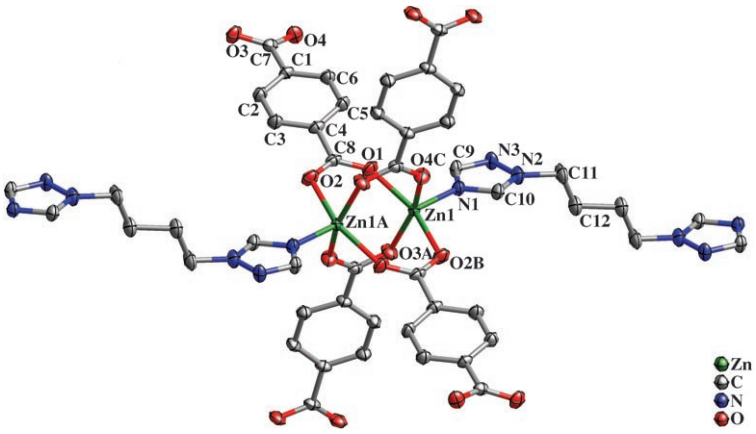

Figure 5. ORTEP diagram showing the coordination environment for a paddle-wheel cluster in **2**.

twofold,[17] and only a few threefold interpenetrated frameworks have been identified until now.[18]

When oba, a flexible dicarboxylate ligand, is used instead of rigid bdc, a new (3,4)-connected 3D interpenetrating network with an unprecedented topology is produced. In the crystal structure of **3**, there is one Zn^{II} atom, one oba ligand, and half an L ligand in the asymmetric unit. Each Zn^{II} atom in **3** is bonded by two oxygen atoms from the two μ-carboxylate ends of two oba ligands (Zn–O 1.966(3) and 1.990(3) Å), two oxygen atoms of one chelating carboxylate end of one oba ligand (Zn–O 2.029(3) and 2.266(3) Å), and one nitrogen atom (Zn–N 2.026(3) Å) of an L ligand to furnish an approximately trigonal bipyramidal geometry (Figure 9). Two Zn atoms related by a twofold axis are bridged by a pair of the oba μ-carboxylate ends into a dinuclear unit with a Zn···Zn distance of 3.553(3) Å. A face-to-face distance of 3.35 Å between a pair of oba ligands coordinated to the two Zn^{II} atoms is observed, showing significant intramolecular π–π interactions (see Figure S5 in the Supporting information). The V-shaped oba ligands (dihedral angle ≈76° between two phenyl rings) link the adjacent dinuclear units in the chelate-bidentate coordination mode (see Figure 10d) into a neutral layer of composition [Zn(oba)] (Figure 11a). Considering the Zn atoms and

bonded to each Zn center via a nitrogen atom. Thus, an arrangement where the carboxylate carbon atoms and triazolyl nitrogen atoms are linked in turn constitutes an octahedral SBU $[Zn_2(CO_2)_4N_2]$ (Figure 2, middle). Each octahedral SBU, which acts as a node, is connected to six others through four bridging bdc and two L ligands (see Figure S3 in the Supporting information) to generate an extended neutral 3D network (see Figure S4 in the Supporting information), which can also be considered as being constructed from distorted 2D square-grid (4,4) layers of composition [Zn(bdc)] pillared by the long L ligands (Figure 6). The overall topology of the 3D frame is best described as a compressed α-Po net based on three intersecting (4,4) nets that possesses large distorted cube-like cavities of approximately 11 Å × 11 Å × 17 Å (Figure 7). The large voids formed by a single 3D network allow incorporation of other two identical networks, thus giving a threefold interpenetrated α-Po-related network that belongs to Class Ia (all the interpenetrated nets are generated only by translation and the translating vector is [100] (7.66 Å)), as shown in Figure 8. The essence of the interpenetration is that the second and third nets are located, equally spaced, along the rhombohedral "solid diagonal" of a distorted cube of the first net. Given that the α-Po net is self-dual,[16] it is not surprising to find pairs of such nets interpenetrating. However, we noticed that among the currently known examples of α-Po topology the majority are

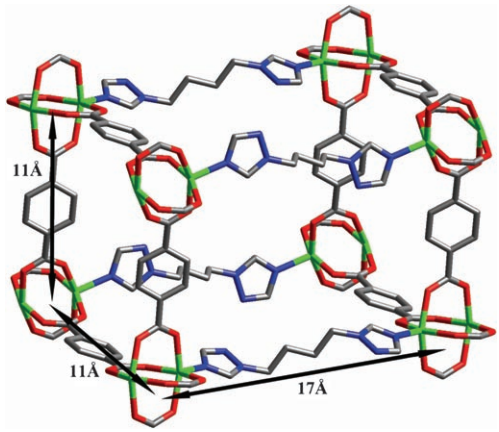

Figure 7. A single distorted cube-like unit of a single α-Po net in **2** with the relative dimensions 11 × 11 × 17 Å^3.

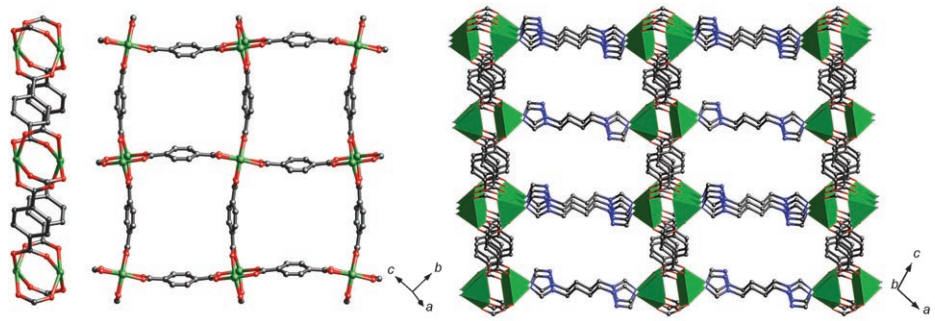

Figure 6. Side and front views of one (4,4) layer (left and middle) and a single 3D network pillared by L ligands in **2** (right).

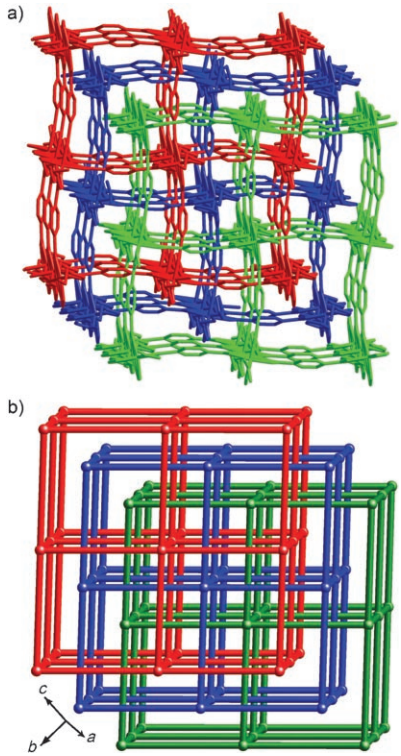

Figure 8. a) Perspective and b) schematic views of the threefold interpenetrating α-Po network of **2**.

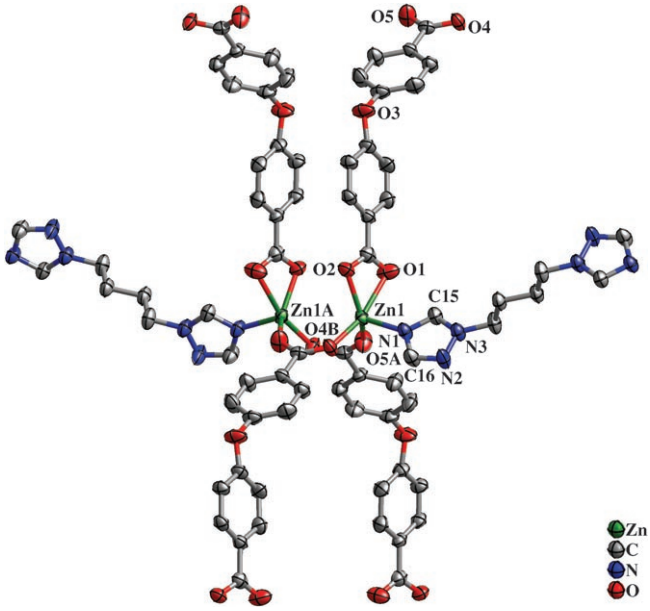

Figure 9. ORTEP diagram showing the coordination environment for a dinuclear zinc unit in **3**.

the C atoms of the μ-carboxylate groups as nodes, we can see that the layers comprise honeycomb-like meshes with a three-connected ($4{\cdot}10^2$) topology that is rare if compared with layers that show the more common square (4^4) or hexagonal (6^3) topologies (Figure 11b). Just like **2**, these 2D

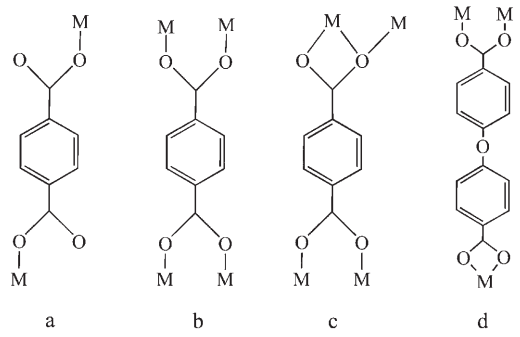

Figure 10. Coordination modes of aromatic dicarboxylic ligands in **1**–**4**.

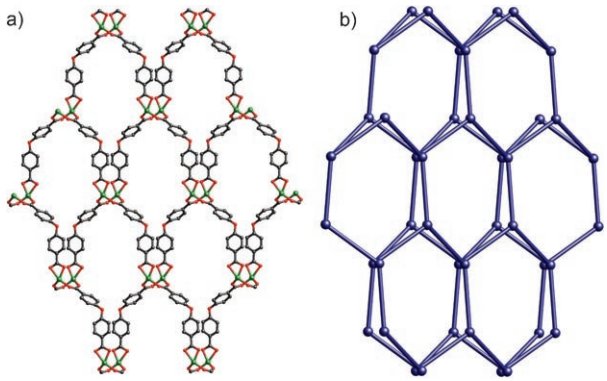

Figure 11. A neutral three-connected layer of composition [Zn(oba)]: a) with a ($4{\cdot}10^2$) topology b) in **3**.

sheets are further connected together in the third dimension by axially coordinating L ligands to give a unique (3,4)-connected 3D framework (see Figure S6 in the Supporting information) with an unprecedented topology of ($4{\cdot}6{\cdot}10$)-($4{\cdot}6^2{\cdot}10^3$), though a large number of possible (3,4)-connected 3D nets have been reported. No fewer than 30 topologically nonuniform examples were listed by Wells.[19] In this simplification the four-connected nodes are the single metals and the three-connected ones are the carbon atoms of the oba ligands bridging on the bimetallic unit (see Figure 12, route I, and Figure S7 in the Supporting information). Interestingly, an individual 3D framework possesses three-directional open channels of approximately 13.9 Å × 14.7 Å along the *a* axis, of 8.3 Å × 13.9 Å along the *b* axis, and of 8.3 Å × 8.3 Å along the *c*-axis (see Figure S8 in the Supporting information). As a consequence of Mother Nature's horror vacui, **3** adopts threefold interpenetration to avoid extremely large void spaces, with a translation vector corresponding to the crystallographic *c* axis (11.39 Å) (Figure 13). Significant intra- (mentioned above) and internetwork π–π (interplanar distance 3.65 Å) and C–H···π (edge-to-face separation 3.77 Å) supramolecular interactions between the aromatic rings contained in this structure presumably help to stabilize the structure adopted. However, in spite of interpenetration, **3** still possesses free void space in the [0 0 1] direction estimated to be about 1011.5 $Å^3$, that is, 24.1% of the crystal volume (Figure 14).

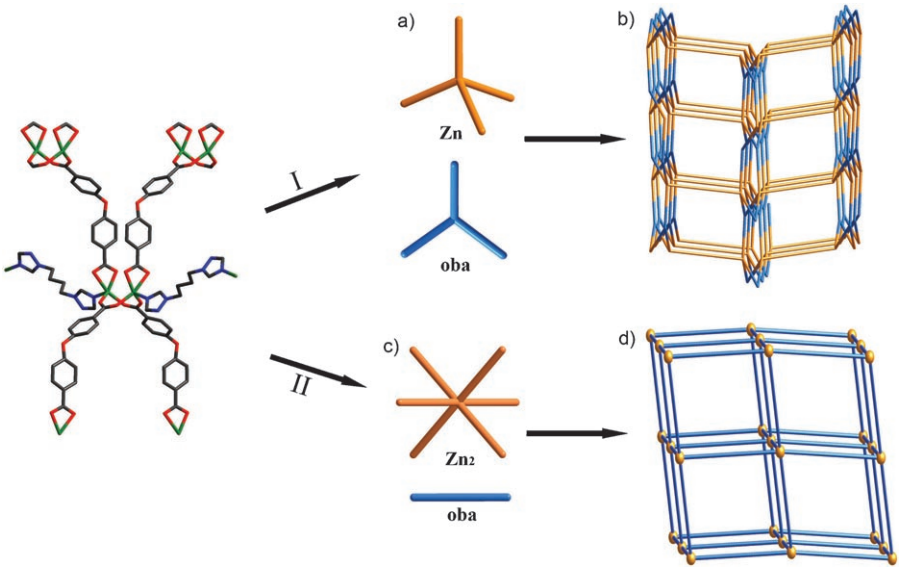

Figure 12. The two simplified models applied in the topological analysis of **3**. I: single metal as a four-connected node and oba ligand as three-connected node. II: bimetallic unit as a six-connected node and all ligands as linear linkers.

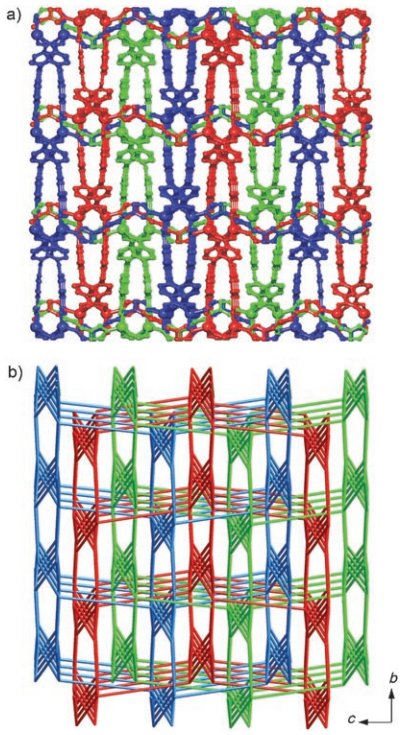

Figure 13. a) Perspective and b) schematic views of the threefold interpenetrating (3,4)-connected net of $(4\cdot6\cdot10)(4\cdot6^2\cdot10^3)$ topology of **3**.

Interestingly, if the dinuclear units are drastically simplified to their baricenters (new six-connected nodes) joined by four oba and two L ligands (new linear links), an alternative rationalization is possible that is closely related to that of **2**, a threefold interpenetrated six-connected net with α-Po topology (see Figure 12, route II, and Figures S7 and S9 in the Supporting information).

When Zn^{II} is replaced with Cd^{II}, which is larger, a particularly fascinating structure is obtained. Compound **4** exhibits the rare 3D self-penetrating network with an unprecedented $4^{20}6^8$ topology. The structure of **4** consists of trinuclear cadmium clusters, in which 1.5 crystallographically independent Cd^{II} atoms exhibit different coordination spheres, although both are eight-coordinate. One Cd^{II} center (Cd1) lies on a center of symmetry and is coordinated to six carboxylic oxygen atoms from six different bdc ligands (Cd–O 2.2666(19)–2.3152(16) Å) (Figure 15). The other Cd^{II} center (Cd2) is ligated with four carboxylic oxygen atoms (Cd–O 2.2256(19)–2.4417(17) Å) from three bdc ligands, one nitrogen atom from an L ligand (Cd–N 2.281(2) Å), and an aqua ligand

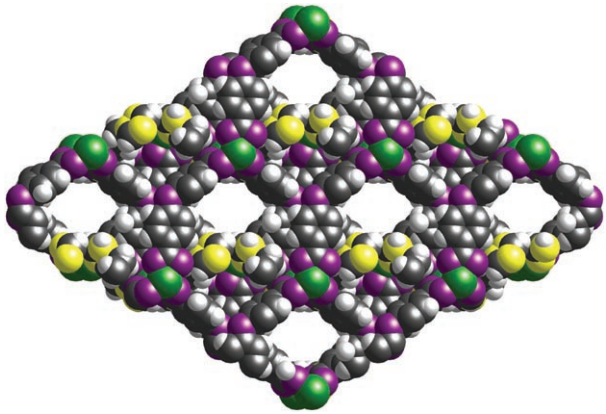

Figure 14. The packing down the *c* axis in **3**, showing the main channels.

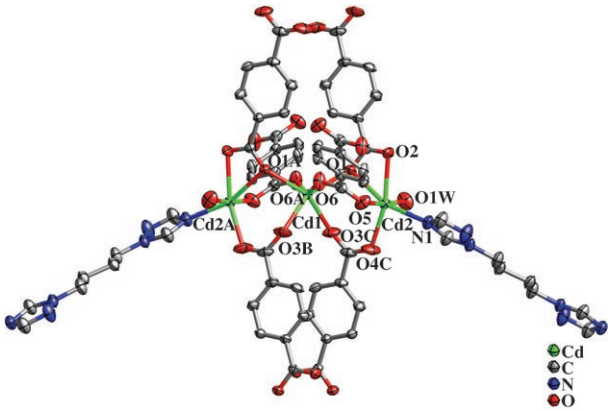

Figure 15. ORTEP diagram showing the coordination environments around the cadmium atoms in **4**.

($Cd-O_{ow}$ 2.308(2) Å). The octahedrally coordinated Cd1 is connected to two adjacent Cd2 centers in a corner-sharing mode to form a $[Cd_3(\mu_3\text{-}O)_2]^{6+}$ core via μ_3-carboxylate atoms (O1) with a nonbonding Cd···Cd distance of 3.6102(11) Å (Figure 2, right). As far as we know, only a few $[Cd_3(\mu_3\text{-}OH)]^{5+}$ cores have been reported to date.[20] As illustrated in Figure 16, there are eight organic ligands (six

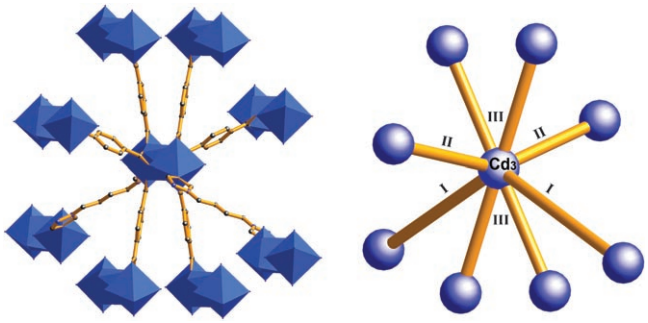

Figure 16. Perspective (left) and simplified (right) views of the eight-connecting trinuclear cadmium cluster. The symbols of three types of linkers are I (20.33 Å), II (11.82 Å), and III (10.87 Å), respectively.

bdc and two L) surrounding each Cd_3 unit. This, therefore, defines an eight-connected node which is further linked to eight nearest neighbors at distances of 10.87–20.33 Å through eight bridging ligands. This process, when repeated, results in a unique 3D uninodal framework of $4^{20}6^8$ topology with eight-connecting trinuclear cadmium clusters as nodes (Figure 17). The eight-connecting framework topology, to

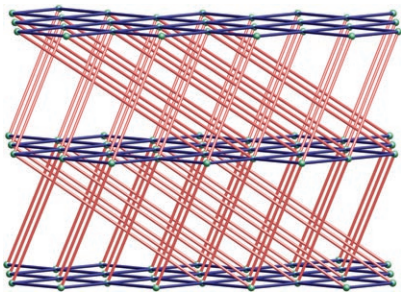

Figure 17. Topological representation of **4** showing the $4^{20}6^8$ topology. The trinuclear cadmium clusters are represented by balls.

our knowledge, is completely new within coordination polymer chemistry. The discovery of this new topology is useful at the basic level in the crystal engineering of coordination networks. According to the new approaches to the analysis of highly connected frameworks proposed by Hill et al.,[21] namely visualization of the structures as combinations of interconnected 2D subnet tectons, the eightfold connectivity of the structure of **4** can be described as being formed from parallel 4^4 nets (in the crystallographic (001) plane with a node–node distance of 10.87 Å), with each center providing four links (11.82 and 20.33 Å long) to four different centers in adjacent nets, two on each side (Figure 17).

Notably, the structure of **4** is completely different from that of the familiar body-centered cubic lattice (bcu).[22] As shown in Figure 18, the parallel (4,4) nets of both bcu and **4** are crosslinked by zigzag chains; however, the detailed con-

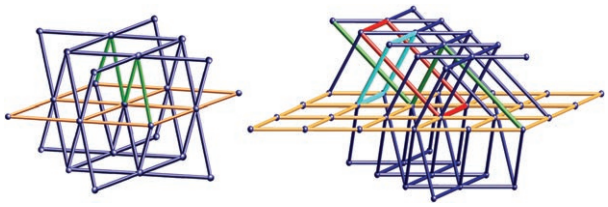

Figure 18. Schematic representations illustrating the different links between the 4^4 nets in the eight-connected nets of bcu (left) and **4** (right). The self-penetrating shortest circuits are highlighted.

nection modes are different. In bcu the zigzag chain in the interlayer region bridges across the diagonal of a single window in the (4,4) net (Figure 18, left). In **4**, however, it bridges the diagonal of six windows (Figure 18, right). Such an unusual linkage mode is also distinct from a previously known non-bcu eight-connected net,[23] in which the zigzag chains bridge the edges of one (4,4) net and the diagonal of the next. As a result of this unique bridging of parallel layers, the catenated four-membered shortest rings (that is, each four-membered ring is interlocked with four others of different sizes at one time) are observed at the intersection of the crossing of two-dimensional layers (Figure 17, and Figure S10 in the Supporting information). Therefore, the resulting array is a single eight-connected self-penetrating network.

A better insight into the nature of this intricate architecture can be achieved if one can imagine removing one at a time from the three types of links of different lengths (see Figure 16, right). On removing type I (20.33 Å) or II (11.82 Å), both of the remainders are three-dimensional six-connected frames with the distorted α-Po topology (Figure 19a,b). However, elimination of type III (10.87 Å) leaves a three-dimensional four-connected frame based upon tetrahedral nodes, exhibiting an intriguing fivefold interpenetrating diamond-like substructure (Figure 19c, and Figure S11 in the Supporting information). For any *n*-fold interpenetrated net, it is always true that if the extra edges that could connect all the *n*-fold interpenetrated nets together are added, a single self-penetrating net with higher connectivity/coordination will be obtained. Therefore, the overall framework of **4** is clearly a self-penetrating net and can be considered as derived from five interpenetrating diamond-like nets that are crosslinked by four extra connections (namely type III) parallel to the (001) plane from each node (see Figure 20 and Figure S12 in the Supporting information).

As stated by O'Keeffe, "MOFs based on nets with coordination numbers = 8[24] are rare and we do not expect structures built from SBUs with eight vertices to be very common."[25] To our knowledge, the very few known eight-connected species within coordination polymers are either single[23,26a,b] or interpenetrating.[26c,d] The sole eight-connect-

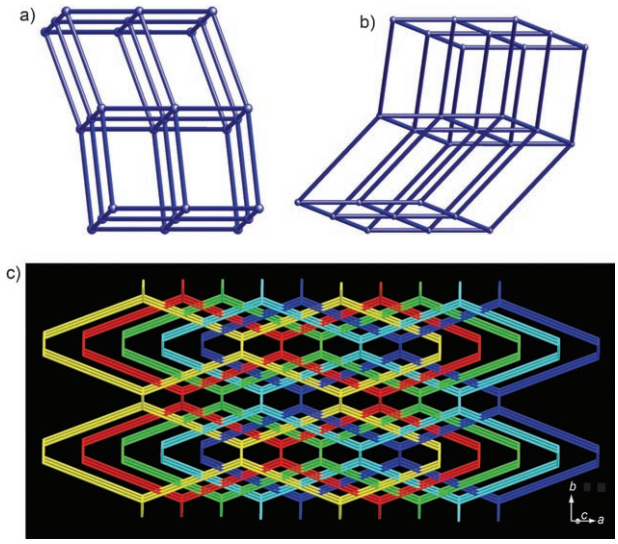

Figure 19. a, b) The results of eliminating type I or II linkers that leave three-dimensional frames with the α-Po topology; c) the result of removing type III that leads to a fivefold interpenetrating diamondoid-like frame.

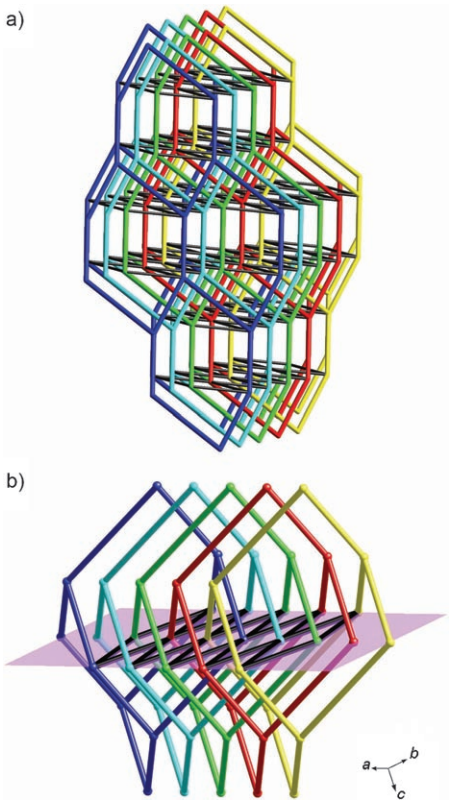

Figure 20. a) The eight-connected self-penetrating net derived from five interpenetrating diamondoid nets; b) the amplified links crossing the five interpenetrating diamondoid nets.

ed self-penetrating network entirely sustained by the coordinative bonds is the complex $[Zn_5(\mu_3\text{-}OH)_2(bdc)_4(phen)_2]$ (phen = 1,10-phenanthroline) reported by us very recently,[27] in which two interpenetrating α-Po nets are crosslinked by two extra connections from each node along the cube diagonals (Figure S13 in the Supporting information). The topology ($4^{24}\cdot5\cdot6^3$) is significantly different from that of the coordination polymer described here. Therefore, to the best of our knowledge, the framework reported herein defines a new topology for eight-connected coordination networks, and represents the highest connected topology at present known for self-penetrating systems.

Thermal properties: To study the thermal stability of **1**–**4**, thermogravimetric (TG) analyses were performed on polycrystalline samples under a nitrogen atmosphere (Figures S14–S17 in the Supporting information). Complex **1** first lost weight corresponding to two isolated water molecules (observed 4.19%, calculated 4.07%) from 85 to 140°C, leaving a framework of $Zn_2(bdc)_2(L)_2$. This framework was stable up to 350°C; decomposition of organic components occurred between 350°C and 800°C (obsd 76.56%, calcd 77.06%). The remaining weight (19.25%) indicated that the final product was ZnO (calcd 18.87%).

The TG curves of **2** and **3** are very alike, consistently with their similar structural skeleton. No weight losses were observed for either compound up to 345°C; above 345°C, significant weight losses occurred and ended at ≈530°C, indicating complete decomposition of the complexes to form ZnO as a final product. This conclusion is supported by the percentages of the residues (26.04% for **2** and 19.58% for **3**), which are in accordance with the expected values (25.53% and 19.91% for **2** and **3**, respectively).

The TG curve of **4** exhibits three well-separated weight loss stages. The first, of 3.16% from 190 to 220°C, corresponds to the loss of two coordinated water molecules (calcd 3.40%). The second, of 15.53% from 220 to 320°C, is equivalent to the loss of one bdc ligand (calcd 15.48%). The third, of 44.21% from 345 to 600°C, is consistent with removal of the remaining two bdc and two L ligands (calcd 45.05%). The remaining weight (36.26%) corresponds to the percentage (36.91%) of Cd and O components in CdO, indicating that this is the final product.

Luminescent properties: Upon excitation of **1**–**4** in the solid state at room temperature, intense bands in the emission spectra are observed at 475 nm (λ_{ex} = 422 nm) for **1**, 465 nm (λ_{ex} = 420 nm) for **2**, 462 nm (λ_{ex} = 425 nm) for **3**, and 435 nm (λ_{ex} = 370 nm) for **4** (Figure 21). As reported previously,[28] solid H_2oba and H_2bdc ligands are nearly nonfluorescent in the range 400–800 nm for excitation wavelengths between 360 and 450 nm at ambient temperature. To understand more thoroughly the nature of the emission band, investigation revealed that the ligand **L** displayed no luminescence. From the theoretical viewpoint, because of the impact of the relativistic effect, the coordination structures, and electron correlation effects, the $(n+1)$ s orbitals of the d^{10} metals contract and therefore have lower energies.[29,30] In these complexes, the highest occupied molecular orbitals (HOMOs) are presumably associated with the π-bonding orbitals from aromatic rings, whereas the lowest un-

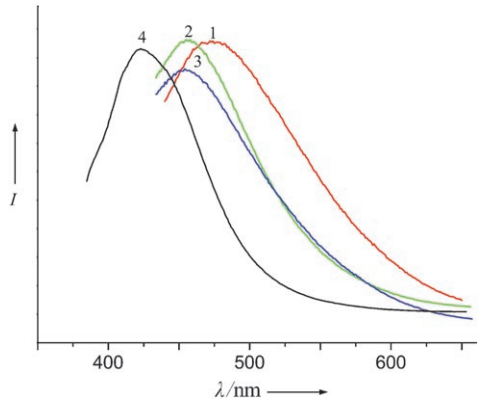

Figure 21. Emission spectra of **1**–**4** in the solid state at room temperature.

occupied molecular orbitals (LUMOs) are associated mainly with the Zn/Cd–O(carboxy) σ^*-antibonding orbitals, localized more on the metal centers. Thus the origin of the emission might be attributable to ligand-to-metal charge transfer (LMCT).[31] The enhancement of luminescence in d^{10} complexes may be attributed to ligand chelation to the metal center which effectively increases the rigidity of the ligand and reduces the loss of energy by radiationless decay.[32] These observations indicate that these condensed polymeric materials may be excellent candidates for potential photoactive materials, since they are thermally stable and insoluble in common polar and nonpolar solvents.

Discussion

As shown above, the simultaneous use of the flexible long-chain ligand L and aromatic dicarboxylate ligands affords various entangled architectures. Although we are unable to propose definitive reasons as to why each compound adopts a different topology with our present state of knowledge, some of the general trends observed are discussed below.

Effect of metal nuclearity: The connectivities of the four compounds are strongly related to the metal nuclearity. The following discussion offers a qualitative explanation for this conclusion. As described above, in **1** all the metal atoms exist only in a mononuclear fashion and are coordinated by four nonplanar bridging ligands to serve as four-connected nodes, finally resulting in a typically four-connected diamondoid network. In contrast to **1**, **2**, and **3** both contain dinuclear metal units. When considered as a whole, they act as six-connected nodes to form three-dimensional six-connected frameworks, whereas in **4** single metal atoms are substituted by trinuclear metal clusters to form eight-connected nodes, giving an unusual eight-connected framework. From the regular trend observed for **1**–**4**, we can see that the increase in metal nuclearity (from 1 to 3) induces the progressive increase in connectivity of the ultimate net (from 4 to 8); in other words, the metal nuclearity plays a significant role in tuning the connectivity of a specific network because metal-cluster based nodes generally have larger surface areas (sometimes even nanoscale) and therefore they can accommodate the steric demands of organic linkers more readily. In a very loose and general sense, the higher the nuclearity of a metal cluster, the more likely is it that a highly connected net is obtained. This therefore provides a promising pathway toward the generation of metal–organic frameworks with unusually high connectivities.

Effect of coordination modes of carboxylate ligands: Multidentate carboxylate ligands have proven to be good candidates for building metal–organic frameworks, owing to their diverse coordination modes.[33] It is instructive to compare the coordination modes of carboxylate ligands in these compounds. In **1**, bdc adopts a bridging *syn–anti* bis(monodentate) coordination mode (Figure 10a), which determines that each metal atom has no choice but to exist in a single-nuclear fashion. In **2** and **3**, whether for the rigid bdc or for the flexible oba ligand, there exists a bis(bidentate) coordination mode, as shown in Figure 10b,d. This mode is essential in chelating metal ions and locking their positions into M–O–C clusters.[34] The most popular is the "paddle-wheel" cluster in which a metal dimer is bridged by four bis(monodentate) carboxylates. Therefore, the formation of the dinuclear units in the two compounds might reasonably be attributed to the bridging *syn–syn* bidentate ends of dicarboxylate ligands, whereas in **4**, apart from the bis(bidentate) binding mode that tends to favor the formation of a dimeric unit, there is a tridentate bridge that is rare in metal–carboxylate complexes (Figure 10c).[35] Such a tridentate bridge mode is postulated to be an important intermediate in "carboxylate-shift" chemistry[35a] and is a key factor for the formation of the trinuclear metal cluster. Thus the coordination modes of carboxylate ligands influence the metal nuclearity and hence the connectivity of the resulting net.

Additional factors, such as the size of metal ions, the stoichiometric ratio of the reactive materials, the reaction pH, and the versatility of the metal coordination geometry, play fundamental roles in the formation of the final product. Since these factors work together to affect the structures, it is difficult to separate and rationalize them.

Conclusion

The simultaneous use of the flexible long-chain ligand L and aromatic dicarboxylate ligands to react with d^{10} metals affords a variety of interesting self-assembled polymeric architectures providing new examples of entangled systems, illustrating again the aesthetic diversity of coordinative network chemistry. Topological analyses of the four complexes indicate that symmetrical and simple SBUs such as tetrahedra in **1** and octahedra in **2** and **3** are liable to lead to predictable topologies, whereas complex and uncommon SBUs as in **4** tend to form previously unobserved topologies. Although it is still difficult to predict the structures accurately, given the well-defined topologies and rigid backbone structures of

metal-cluster based SBUs, we expect assembly of 3D structures to happen in a more controllable manner. The progressive tendency of the connectivity observed for these complexes with an increase in metal nuclearity shows that tuning of metal nuclearity via the coordination modes of carboxylate ligands can influence the connectivity of the resulting networks. It is believed that the preliminary results presented here may also provide a promising pathway to rational design of diversely connected metal–organic frameworks, a goal that we are pursuing actively.

Experimental Section

Materials and physical measurements: All chemicals were purchased commercially and used without further purification. Elemental analyses (C, H, and N) were performed on a Perkin-Elmer 2400 CHN elemental analyzer. IR spectra were recorded in the range 400–4000 cm^{-1} on an Alpha Centaurt FT/IR spectrophotometer using KBr pellets. TG analyses were performed on a Perkin-Elmer TGA7 instrument in flowing N_2 with a heating rate of 10 °C min^{-1}. Excitation and emission spectra were obtained on a SPEX FL-2T2 spectrofluorimeter equipped with a 450 W xenon lamp as the excitation source.

Syntheses

$[Zn_2(bdc)_2(L)_2]\cdot 2H_2O$ (1): A mixture of $Zn(NO_3)_2\cdot 6H_2O$ (149 mg, 0.5 mmol), H_2bdc (83 mg, 0.5 mmol), L (96 mg, 0.5 mmol), and water (10 mL) was placed in a Teflon reactor (23 mL). The pH was adjusted to 5.0 by addition of triethylamine, the mixture was heated at 160 °C for three days, and then it was cooled to room temperature at 10 °C h^{-1}. Colorless crystals of **1** were obtained in 68 % yield based on Zn (150 mg). Elemental analysis (%) calcd: C 43.50, H 4.56, N 19.03; found: C 43.58, H 4.49, N 19.13; IR (KBr): $\tilde{\nu}$ = 3446 (br), 3121(m), 3047(w), 2957(w), 2876(w), 1631(s), 1599(s), 1530(m), 1505(m), 1392(s), 1300(w), 1281(s), 1217(w), 1136(s), 1089(w), 999(s), 895(m), 876(w), 826(s), 792(w), 755(s), 674(m), 657(m), 543(s), 458(w) cm^{-1}.

$[Zn(bdc)(L)_{0.5}]$ (2): A mixture of $Zn(NO_3)_2\cdot 6H_2O$ (149 mg, 0.5 mmol), H_2bdc (83 mg, 0.5 mmol), L (48 mg, 0.25 mmol), and water (10 mL) was placed in a Teflon reactor(23 mL). The pH was adjusted to 7.5 by addition of triethylamine, the mixture was heated at 160 °C for three days, and then it was cooled to room temperature at 10 °C h^{-1}. Colorless crystals of **2** were obtained in 52 % yield based on Zn (85 mg). Elemental analysis (%) calcd: C 44.13, H 3.39, N 12.87; found: C 44.07; H 3.31; N 12.90; IR (KBr): $\tilde{\nu}$ = 3153(m), 3112(w), 3057(w), 2930(w), 2882(w), 1618(s), 1552(s), 1520(m), 1470(m), 1401(s), 1324(m), 1281(s), 1206(w), 1136(s), 1114(w), 989(s), 893(m), 868(w), 832(m), 783(w), 757(s), 673(m), 652(m), 538(s), 462(w) cm^{-1}.

$[Zn(oba)(L)_{0.5}]$ (3): Compound **3** was prepared as for **2** by using H_2oba instead of H_2bdc. Colorless crystals of **3** were obtained in 64 % yield based on Zn (134 mg). Elemental analysis (%) calcd: C 51.63, H 3.61, N 10.04; found: C 51.66, H 3.54, N 10.10; IR (KBr): $\tilde{\nu}$ = 3153(m), 3067(w), 2996(w), 2929(w), 2870(w), 1620(s), 1598(s), 1573(m), 1540(m), 1504(m), 1467(w), 1405(s), 1305(w), 1284(w), 1252(s), 1159(s), 1131(s), 1097(m), 1011(m), 998(s), 884(s), 865(w), 801(m), 776(s), 754(w), 737(w), 709(w), 698(m), 674(w), 663(m), 653(m), 631(w), 618(w), 526(m), 499(w), 444(m) cm^{-1}.

$[Cd_3(bdc)_3(L)_2(H_2O)_2]$ (4): A mixture of $Cd(NO_3)_2\cdot 4H_2O$ (154 mg, 0.5 mmol), H_2bdc (83 mg, 0.5 mmol), L (58 mg, 0.3 mmol), and water (10 mL) was placed in a Teflon reactor (23 mL). The pH was adjusted to 8.0 by addition of triethylamine, the mixture was heated at 160 °C for three days, and then it was cooled to room temperature at 10 °C h^{-1}. Colorless crystals of **4** were obtained in 48 % yield based on Cd (85 mg). Elemental analysis (%) calcd: C 36.26, H 2.85, N 7.93; found: C 36.34, H 2.89, N 7.87; IR (KBr): $\tilde{\nu}$ = 3387 (br), 3412(w), 3112(w), 3067(w), 2948(w), 2881(w), 2667(w), 2552(w), 1678(w), 1649(w), 1573(s), 1521(w), 1505(m), 1374(s), 1318(w), 1286(s), 1208(w), 1136(s), 1113(w), 1091(w), 1116(m), 998(m), 944(w), 898(m), 868(w), 856(w), 833(m), 819(m), 781(m), 747(s), 673(m), 684(m), 530(s), 462(m) cm^{-1}.

Crystal structure determination: Intensity data were collected on a Rigaku R-Axis Rapid IP diffractometer with $Mo_{K\alpha}$ monochromated radiation (λ = 0.71073 Å) at 293 K. Empirical absorption correction was applied. The structures of **1–4** were solved by the direct method and refined by the full-matrix least squares on F^2 using the SHELXL-97 software.[36] All of the non-hydrogen atoms were refined anisotropically. The organic hydrogen atoms were generated geometrically; the aqua hydrogen atoms were located from difference maps and refined with isotropic temperature factors. Crystal data and structure refinement for **1–4** are summarized in Table 1. Selected bond lengths and angels of **1–4** are listed in Table 2.

Table 1. Crystal data and structure refinements for complexes **1–4**.

	1	**2**	**3**	**4**
formula	$C_{32}H_{40}N_{12}O_{10}Zn_2$	$C_{12}H_{11}N_3O_4Zn$	$C_{18}H_{15}N_3O_5Zn$	$C_{32}H_{30}N_6O_{14}Cd_3$
M_r [g]	883.50	326.61	418.70	1059.82
crystal system	triclinic	monoclinic	monoclinic	monoclinic
space group	$P\bar{1}$	$P2_1/n$	$C2/c$	$C2/c$
a [Å]	9.6551(19)	7.6645(15)	14.747(3)	7.9993(16)
b [Å]	11.322(2)	15.508(3)	25.414(5)	20.206(4)
c [Å]	18.200(4)	11.242(2)	11.387(2)	21.281(4)
α [°]	98.90(3)	90	90	90
β [°]	91.04(3)	103.68(3)	100.65(3)	91.19(3)
γ [°]	111.01(3)	90	90	90
V [$Å^3$]	1829.0(6)	1298.4(4)	4194.2(15)	3439.0(12)
Z	2	4	8	4
ρ_{calcd} [g cm^{-3}]	1.604	1.671	1.326	2.047
μ [mm^{-1}]	1.386	1.908	1.201	1.919
collected reflections	14183	12559	19991	16730
unique reflections (R_{int})	6370(0.0535)	2967(0.0401)	4773(0.0597)	3932(0.0276)
observed reflections [$I>2\sigma(I)$]	4246	2635	3819	3681
refined parameters	505	181	244	251
goodness of fit	1.063	0.882	1.030	1.079
R_1[a]/wR_2[b] [$I>2\sigma(I)$]	0.0619/0.1482	0.0291/0.0707	0.0495/0.1603	0.0213/0.0489
R_1[a]/wR_2[b] (all data)	0.0961/0.1689	0.0342/0.0739	0.0622/0.1701	0.0236/0.0495
largest residuals [e $Å^{-3}$]	1.207/−0.557	0.371/−0.494	0.857/−0.444	0.546/−0.557

[a] $R_1 = \Sigma||F_0|-|F_c||/\Sigma|F_0|$. [b] $wR_2 = \Sigma[w(F_0^2-F_c^2)^2]/\Sigma[w(F_0^2)^2]^{1/2}$.

Table 2. Selected bond lengths [Å] and angles [°] for **1**–**4**.[a]

complex **1**			
Zn1−O4	1.963(4)	Zn2−O7	1.936(4)
Zn1−O2	2.002(5)	Zn2−O5	1.986(4)
Zn1−N7	2.009(4)	Zn2−N4	2.017(4)
Zn1−N10	2.059(4)	Zn2−N3	2.046(4)
O4-Zn1-O2	111.1(2)	O4-Zn1-N7	120.52(19)
O2-Zn1-N7	113.9(2)	O4-Zn1-N10	100.46(18)
O2-Zn1-N10	96.1(2)	N7-Zn1-N10	111.00(18)
O7-Zn2-O5	104.08(19)	O7-Zn2-N4	96.81(18)
O5-Zn2-N4	126.12(19)	O7-Zn2-N3	120.4(2)
O5-Zn2-N3	99.14(18)	N4-Zn2-N3	111.92(18)
Complex **2**			
Zn1−N1	2.0145(18)	Zn1−O3A	2.0445(16)
Zn1−O2B	2.0498(16)	Zn1−O4C	2.0516(16)
Zn1−O1	2.0670(16)		
N1-Zn1-O3A	100.40(7)	N1-Zn1-O2B	104.02(7)
O3A-Zn1-O2B	87.60(7)	N1-Zn1-O4C	101.54(7)
O3A-Zn1-O4C	158.06(7)	O2B-Zn1-O4C	87.05(7)
N1-Zn1-O1	97.47(7)	O3A-Zn1-O1	90.10(7)
O2B-Zn1-O1	158.45(7)	O4C-Zn1-O1	87.14(7)
complex **3**			
Zn1−O5A	1.966(3)	Zn1−O4B	1.990(2)
Zn1−N1	2.026(3)	Zn1−O2	2.029(3)
Zn1−O1	2.266(3)		
O5A-Zn1-O4B	102.10(13)	O5A-Zn1-N1	105.97(13)
O4B-Zn1-N1	96.71(12)	O5A-Zn1-O2	131.58(14)
O4B-Zn1-O2	102.57(11)	N1-Zn1-O2	111.67(13)
O5A-Zn1-O1	89.44(13)	O4B-Zn1-O1	163.44(12)
N1-Zn1-O1	91.37(13)	O2-Zn1-O1	60.93(11)
complex **4**			
Cd1−O6	2.2572(17)	Cd1−O6A	2.2573(17)
Cd1−O3B	2.2666(19)	Cd1−O3C	2.2666(19)
Cd1−O1	2.3151(16)	Cd1−O1A	2.3152(16)
Cd2−O4C	2.2256(19)	Cd2−O5	2.2295(17)
Cd2−N1	2.281(2)	Cd2−O1W	2.308(2)
Cd2−O2	2.3394(18)	Cd2−O1	2.4417(17)
O6-Cd1-O6A	148.00(12)	O6-Cd1-O3B	85.85(8)
O6-Cd1-O1	82.13(7)	O6A-Cd1-O1	82.32(7)
O3B-Cd1-O1	151.66(7)	O3C-Cd1-O1	82.09(7)
O1-Cd1-O1A	121.24(8)	O4C-Cd2-O(5)	95.00(8)
O4C-Cd2-N1	89.50(8)	O5-Cd2-N1	95.04(7)
N1-Cd2-O1W	90.10(8)	O4C-Cd2-O2	162.60(7)
O5-Cd2-O2	88.09(7)	N1-Cd2-O2	107.31(7)
O1W-Cd2-O1	80.63(7)	O2-Cd2-O1	54.66(6)

[a] Symmetry operations: for **2**: A) $-x-1/2$, $y+1/2$, $-z+3/2$; B) $-x$, $-y+2$, $-z+1$; C) $x+1/2$, $-y+3/2$, $z-1/2$; for **3**: A) $-x+3/2$, $y-1/2$, $-z+1/2$; B) $x-1/2$, $y-1/2$, z; for **4**: A) $-x+2$, y, $-z+3/2$; B) $x+1/2$, $y-1/2$, z; C) $-x+3/2$, $y-1/2$, $-z+3/2$.

CCDC-285598 (**1**), CCDC-285599 (**2**), CCDC-285600 (**3**), and CCDC-285601 (**4**) contain the supplementary crystallographic data for this paper. These data can be obtained free of charge from the Cambridge Crystallographic Data Centre via www.ccdc.cam.ac.uk/data_request/cif.

Acknowledgements

The authors thank the National Natural Science Foundation of China (20371011) for financial support.

[1] a) P. J. Hagrman, D. Hagrman, J. Zubieta, *Angew. Chem.* **1999**, *111*, 2798; *Angew. Chem. Int. Ed.* **1999**, *38*, 2638; b) A. N. Khlobystov, A. J. Blake, N. R. Champness, D. A. Lemenovskii, A. G. Majouga, N. V. Zyk, M. Schröder, *Coord. Chem. Rev.* **2001**, *222*, 155; c) R. Robson, *J. Chem. Soc. Dalton Trans.* **2000**, 3735; d) B. Moulton, M. J. Zaworotko, *Chem. Rev.* **2001**, *101*, 1629; e) M. J. Zaworotko, *Chem. Commun.* **2001**, 1; f) O. M. Yaghi, M. O'Keeffe, N. W. Ockwig, H. K. Chae, M. Eddaoudi, J. Kim, *Nature* **2003**, *423*, 705; g) N. W. Ockwig, O. Delgado-Friederichs, M. O'Keeffe, O. M. Yaghi, *Acc. Chem. Res.* **2005**, *38*, 176.

[2] a) M. Fujita, Y. J. Kwon, S. Washizu, K. Ogura, *J. Am. Chem. Soc.* **1994**, *116*, 1151; b) G. B. Gardner, D. Venkataraman, J. S. Moore, S. Lee, *Nature* **1995**, *374*, 792; c) J. S. Seo, D. Whang, H. Lee, S. I. Jun, J. Oh, Y. J. Jeon, K. Kim, *Nature* **2000**, *404*, 982; d) C. J. Kepert, T. J. Prior, M. J. Rosseinsky, *J. Am. Chem. Soc.* **2001**, *123*, 10001; e) O. R. Evans, W. Lin, *Acc. Chem. Res.* **2002**, *35*, 511; f) C. Janiak, *Dalton Trans.* **2003**, 2781; g) N. L. Rosi, J. Eckert, M. Eddaoudi, D. T. Vodak, J. Kim, M. O'Keeffe, O. M. Yaghi, *Science* **2003**, *300*, 1127; h) S. Kitagawa, R. Kitaura, S. I. Noro, *Angew. Chem.* **2004**, *116*, 2388; *Angew. Chem. Int. Ed.* **2004**, *43*, 2334.'

[3] *Molecular Catenanes, Rotaxanes and Knots, A Journey Through the World of Molecular Topology* (Eds.: J. P. Sauvage, C. Dietrich-Buchecker), Wiley-VCH, Weinheim, **1999**.

[4] a) L. Carlucci, G. Ciani, D. M. Proserpio, *Coord. Chem. Rev.* **2003**, *246*, 247; b) L. Carlucci, G. Ciani, D. M. Proserpio, *CrystEngComm* **2003**, *5*, 269; c) S. A. Bourne, J. Lu, B. Moulton, M. J. Zaworotko, *Chem. Commun.* **2001**, 861; d) X. H. Bu, M. L. Tong, H. C. Chang, S. Kitagawa, S. R. Batten, *Angew. Chem.* **2004**, *116*, 194; *Angew. Chem. Int. Ed.* **2004**, *43*, 192; e) K. Liang, H. Zheng, Y. Song, M. F. Lappert, Y. Li, X. Xin, Z. Huang, J. Chen, S. Lu, *Angew. Chem.* **2004**, *116*, 5900; *Angew. Chem. Int. Ed.* **2004**, *43*, 5776.

[5] a) S. R. Batten, R. Robson, *Angew. Chem.* **1998**, *110*, 1558; *Angew. Chem. Int. Ed.* **1998**, *37*, 1460; b) S. R. Batten, *CrystEngComm* **2001**, *3*, 67.

[6] V. A. Blatov, L. Carlucci, G. Ciani, D. M. Proserpio, *CrystEngComm* **2004**, *6*, 377.

[7] a) B. F. Abrahams, M. J. Hardie, B. F. Hoskins, R. Robson, E. E. Sutherland, *J. Chem. Soc. Chem. Commun.* **1994**, 1049; b) L. Carlucci, G. Ciani, D. M. Proserpio, F. Porta, *Angew. Chem.* **2003**, *115*, 331; *Angew. Chem. Int. Ed.* **2003**, *42*, 317; c) P. Jensen, D. J. Price, S. R. Batten, B. Moubaraki, K. S. Murray, *Chem. Eur. J.* **2000**, *6*, 3186; d) B. F. Abrahams, S. R. Batten, M. J. Grannas, H. Hamit, B. F. Hoskins, R. Robson, *Angew. Chem.* **1999**, *111*, 1538; *Angew. Chem. Int. Ed.* **1999**, *38*, 1475; e) M. A. Withersby, A. J. Blake, N. R. Champness, P. A. Cooke, P. Hubberstey, M. Schröder, *J. Am. Chem. Soc.* **2000**, *122*, 4044; f) M. L. Tong, X. M. Chen, S. R. Batten, *J. Am. Chem. Soc.* **2003**, *125*, 16170; g) L. Carlucci, G. Ciani, D. M. Proserpio, S. Rizzato, *J. Chem. Soc. Dalton Trans.* **2000**, 3821; h) D. L. Long, R. J. Hill, A. J. Blake, N. R. Champness, P. Hubberstey, C. Wilson, M. Schröder, *Chem. Eur. J.* **2005**, *11*, 1384.

[8] a) M. Fujita, O. Sasaki, K. Watanabe, K. Ogura, K. Yamaguchi, *New J. Chem.* **1998**, *22*, 189; b) L. Carlucci, G. Ciani, M. Moret, D. M. Proserpio, S. Rizzato, *Angew. Chem.* **2000**, *112*, 1566; *Angew. Chem. Int. Ed.* **2000**, *39*, 1506.

[9] a) J. P. Sauvage, *Acc. Chem. Res.* **1998**, *31*, 611; b) K. Kim, *Chem. Soc. Rev.* **2002**, *31*, 96.

[10] a) X. L. Wang, C. Qin, E. B. Wang, L. Xu, Z. M. Su, C. W. Hu, *Angew. Chem.* **2004**, *116*, 5146; *Angew. Chem. Int. Ed.* **2004**, *43*, 5036; b) X. L. Wang, C. Qin, E. B. Wang, Y. G. Li, Z. M. Su, L. Xu, L. Carlucci, *Angew. Chem.* **2005**, *117*, 5974; *Angew. Chem. Int. Ed.* **2005**, *44*, 5824; c) C. Qin, X. L. Wang, L. Carlucci, M. L. Tong, E. B. Wang, C. W. Hu, L. Xu, *Chem. Commun.* **2004**, 1876; d) X. L. Wang, C. Qin, E. B. Wang, Y. G. Li, Z. M. Su, *Chem. Commun.* **2005**, 5450.

[11] a) Z. Y. Fu, X. T. Wu, J. C. Dai, L. M. Wu, C. P. Cui, S. M. Hu, *Chem. Commun.* **2001**, 1856; b) L. Carlucci, G. Ciani, D. M. Proserpio, S. Rizzatio, *Chem. Eur. J.* **2002**, *8*, 1520; c) P. Ayyappan, O. R. Evans, W. Lin, *Inorg. Chem.* **2002**, *41*, 3328; d) K. Biradha, M. Fujita, *Chem. Commun.* **2002**, 1866; e) Y. H. Li, C. Y. Su, A. M. Goforth, K. D. Shimizu, K. D. Gray, M. D. Smith, H. C. zur Loye, *Chem. Commun.* **2003**, 1630; f) L. Carlucci, G. Ciani, D. M. Proserpio, *Chem. Commun.* **2004**, 380.

[12] a) S. P. Watton, P. Fuhrmann, L. E. Pence, A. Caneschi, A. Cornia, G. L. Abbati, S. J. Lippard, *Angew. Chem.* **1997**, *109*, 2917; *Angew.*

Chem. Int. Ed. Engl. **1997**, *36*, 2774; b) M. R. Brügstein, M. T. Gamer, P. W. Roesky, *J. Am. Chem. Soc.* **2004**, *126*, 5213.
[13] a) H. Li, M. Eddaoudi, M. O'Keeffe, O. M. Yaghi, *Nature* **1999**, *402*, 276; b) H. Chun, D. Kim. D. N. Dybtsev, K. Kim, *Angew. Chem.* **2004**, *116*, 989; *Angew. Chem. Int. Ed.* **2004**, *43*, 971; c) C. Serre, F. Millange, S. Surblé, G. Férey, *Angew. Chem.* **2004**, *116*, 6445; *Angew. Chem. Int. Ed.* **2004**, *43*, 6285; d) N. Zheng, X. Bu, P. Feng, *Angew. Chem.* **2004**, *116*, 4875; *Angew. Chem. Int. Ed.* **2004**, *43*, 4753; e) B. Kesanli, Y. Cui, M. R. Smith, E. W. Bittner, B. C. Bockrath, W. Lin, *Angew. Chem.* **2005**, *117*, 74; *Angew. Chem. Int. Ed.* **2005**, *44*, 72; f) M. B. Zhang, J. Zhang, S. T. Zheng, G. Y. Yang, *Angew. Chem.* **2005**, *117*, 1409; *Angew. Chem. Int. Ed.* **2005**, *44*, 1385.
[14] a) G. A. van Albada, R. C. Guijt, J. G. Haasnoot, M. Lutz, A. L. Spek, J. Reedijk, *Eur. J. Inorg. Chem.* **2000**, 121; b) Q. H. Zhao, H. F. Li, X. F. Wang, Z. D. Chen, *New J. Chem.* **2002**, *26*, 1709.
[15] C. Janiak, *J. Chem. Soc. Dalton Trans.* **2000**, 3885.
[16] O. D. Friedrichs, M. O'Keeffe, O. M. Yaghi, M. Design, D. Group, *Solid State Sci.* **2003**, *5*, 73.
[17] a) P. C. M. Duncan, D. M. L. Goodgame, S. Menzer, D. J. Williams, *Chem. Commun.* **1996**, 2127; b) E. Siebel, R. D. Fischer, *Chem. Eur. J.* **1997**, *3*, 1987; c) M. Eddaoudi, J. Kim, N. Rosi, D. Vodak, J. Wachter, M. O'Keeffe, O. M. Yaghi, *Science* **2002**, *295*, 469; d) V. Niel, M. C. Munoz, A. B. Gaspar, A. Galet, G. Levchenko, J. A. Real, *Chem. Eur. J.* **2002**, *8*, 2446; e) P. Jensen, S. R. Batten, B. Moubaraki, K. S. Murray, *J. Chem. Soc. Dalton Trans.* **2002**, 3712; f) W. J. Lu, L. P. Zhang, H. B. Song, Q. M. Wang, T. C. W. Mak, *New J. Chem.* **2002**, *26*, 775; g) S. Y. Yang, L. S. Long, Y. B. Jiang, R. B. Huang, L. S. Zheng, *Chem. Mater.* **2002**, *14*, 3229; h) B. F. Abrahams, S. R. Batten, B. F. Hoskins, R. Robson, *Inorg. Chem.* **2003**, *42*, 2654.
[18] a) T. Soma, H. Yuge, T. Iwamoto, *Angew. Chem.* **1994**, *106*, 1746; *Angew. Chem. Int. Ed. Engl.* **1994**, *33*, 1665; b) M. J. Plater, M. R. S. J. Foreman, J. M. S. Skakle, *Cryst. Eng.* **2001**, *4*, 293; c) B. F. Abrahams, B. F. Hoskins, R. Robson, D. A. Slizys, *CrystEngComm* **2002**, *4*, 478.
[19] a) A. F. Wells, *Three-dimensional Nets and Polyhedra*, Wiley-Interscience, New York, **1977**; b) A. F. Wells, *Further Studies of Three-dimensional Nets*, ACA Monograph No. 8, American Crystallographic Association, Pittsburgh, **1979**.
[20] a) M. Weidenbruch, M. Herrndorf, A. Schafer, S. Pohl, W. Saak, *J. Organomet. Chem.* **1989**, *361*, 139; b) T. Konno, Y. Kageyams, K. I. Okamoto, *Bull. Chem. Soc. Jpn.* **1994**, *67*, 1957; c) W. Lin, Z. Wang, L. Ma, *J. Am. Chem. Soc.* **1999**, *121*, 11249; d) X. Xue, X. S. Wang, L. Z. Wang, R. G. Xiong, B. F. Abrahams, X. Z. You, Z. L. Xue, C. M. Che, *Inorg. Chem.* **2002**, *41*, 6544.
[21] R. J. Hill, D. L. Long, N. R. Champness, P. Hubberstey, M. Schröder, *Acc. Chem. Res.* **2005**, *38*, 337.
[22] O. D. Friedrichs, M. O'Keeffe, O. M. Yaghi, *Acta Crystallogr. Sect. A* **2003**, *59*, 22.
[23] D. L. Long, R. J. Hill, A. L. Blake, N. R. Champness, P. Hubberstey, D. M. Proserpio, C. Wilson, M. Schröder, *Angew. Chem.* **2004**, *116*, 1887; *Angew. Chem. Int. Ed.* **2004**, *43*, 1851.
[24] Two twelve-connected nets have just appeared; see: X. M. Zhang, R. Q. Fang, H. S. Wu, *J. Am. Chem. Soc.* **2005**, *127*, 7670; D. Li, T. Wu, X. P. Zhou, R. Zhou, X. C. Huang, *Angew. Chem.* **2005**, *117*, 4247; *Angew. Chem. Int. Ed.* **2005**, *44*, 4175.
[25] O. D. Friedrichs, M. O'Keeffe, O. M. Yaghi, *Acta Crystallogr. Sect. A* **2003**, *59*, 515.
[26] a) D. L. Long, A. J. Blake, N. R. Champness, C. Wilson, M. Schröder, *Angew. Chem.* **2001**, *113*, 2509; *Angew. Chem. Int. Ed.* **2001**, *40*, 2443; b) H. L. Sun, S. Gao, B. Q. Ma, F. Chang, W. F. Fu, *Microporous Mesoporous Mater.* **2004**, *73*, 89; c) L. Pan, H. Liu, X. Lei, X. Huang, D. H. Olsen, N. J. Turro, J. Li, *Angew. Chem.* **2003**, *115*, 560; *Angew. Chem. Int. Ed.* **2003**, *42*, 542; d) Q. Fang, X. Shi, G. Wu, G. Tian, G. Zhu, R. Wang, S. Qui, *J. Solid State Chem.* **2003**, *176*, 1.
[27] X. L. Wang, C. Qin, E. B. Wang, Z. M. Su, L. Xu, S. R. Batten, *Chem. Commun.* **2005**, 4789.
[28] a) J. Tao, J. X. Shi, M. L. Tong, X. X. Zhang, X. M. Chen, *Inorg. Chem.* **2001**, *40*, 6328; b) L. N. Zhu, L. Z. Zhang, W. Z. Wang, D. Z. Liao, P. Cheng, Z. H. Jiang, S. P. Yan, *Inorg. Chem. Commun.* **2002**, *5*, 1017; c) W. Chen, J. Y. Wang, C. Chen, Q. Yue, H. M. Yuan, J. S. Chen, S. N. Wang, *Inorg. Chem.* **2003**, *42*, 944.
[29] a) P. Pyykkö, *Chem. Rev.* **1997**, *97*, 597; b) V. W. W. Yam, K. K. W. Lo, *Chem. Soc. Rev.* **1999**, *28*, 323; c) N. Kaltoyannis, *J. Chem. Soc. Dalton Trans.* **1997**, 1.
[30] K. Balasubramanian, *Relativistic Effects in Chemistry Part A: Theory and Techniques; Part B: Applications*, Wiley, New York, **1997**.
[31] S. L. Zheng, X. M. Chen, *Aust. J. Chem.* **2004**, *57*, 703.
[32] a) S. L. Zheng, J. H. Yang, X. L. Yu, X. M. Chen, W. T. Wong, *Inorg. Chem.* **2004**, *43*, 830; b) B. Valeur, *Molecular Fluorescence: Principles and Applications*, Wiley-VCH, Weinheim, **2002**; c) A. W. Adamson, P. D. Fleischauer, *Concepts of Inorganic Photochemistry*, John Wiley, New York, **1975**; d) H. Yersin, A. Vogler, *Photochemistry and Photophysics of Coordination Compounds*, Springer, Berlin, **1987**.
[33] a) M. Eddaoudi, D. B. Moler, H. Li, B. Chen, T. M. Reineke, M. O'Keeffe, O. M. Yaghi, *Acc. Chem. Res.* **2001**, *34*, 319; b) C. N. R. Rao, S. Natarajan, R. Vaidhyanathan, *Angew. Chem.* **2004**, *116*, 1490; *Angew. Chem. Int. Ed.* **2004**, *43*, 1466; c) G. Férey, C. Mellot-Draznieks, C. Serre, F. Millange, *Acc. Chem. Res.* **2005**, *38*, 217.
[34] J. Kim, B. Chen, T. M. Reineke, H. Li, M. Eddaoudi, D. B. Moler, M. O'Keeffe, O. M. Yaghi, *J. Am. Chem. Soc.* **2001**, *123*, 8239.
[35] a) R. L. Rardin, W. B. Tolman, S. J. Lippard, *New J. Chem.* **1991**, *15*, 417; b) B. H. Ye, X. Y. Li, I. D. Williams, X. M. Chen, *Inorg. Chem.* **2002**, *41*, 6426.
[36] a) G. M. Sheldrick, SHELXS-97, Program for Crystal Structure Solution, University of Göttingen (Germany), **1997**; b) G. M. Sheldrick, SHELXL-97, Program for Crystal Structure Refinement, University of Göttingen (Germany), **1997**.

Received: October 8, 2005
Published online: February 7, 2006

